ENGM224
Geotechnical Engineering 2
Rock Slope Engineering Assignment

Sam Hobbs

April 15, 2013

Contents

List of Figures

List of Tables

1 Introduction

1.1 Objectives

This piece of analysis aims to facilitate the construction of a cutting through sandstone and shale to make way for a new highway. A preliminary rock slope design will be produced, which will include:

- The identification of discontinuity sets.
- Discontinuity set ranking in terms of importance.
- Identification of the most likely failure mechanisms.
- Determination of the best angle within the range 60°-80° for the cut.

The design will also aim to:

- Minimise the amount of land take and volume of rock removal.
- Optimise the design's sustainability and ease of maintenance.
- Recommend slope reinforcement measures where necessary.
- Recommend a suitable excavation methodology for each section of the cutting.
- Identify areas where further investigation is needed for the detailed design, where necessary.

1.2 Scope

The objectives outlined in section 1.1 will be achieved by carrying out the following tasks:

1. Production of a contoured diagram showing the density distribution of poles using a Dimitrijevic and Petrovic (1965) counting net, following the method described by Matherson (1983) (Clayton, Simons, and M. C. Matthews, 1995).
2. Determination of the basic angle of friction for the sandstone using the laboratory test results.
3. Identification of the basic joint sets and ranking in order of importance.
4. Construction of overlays for plane, wedge and toppling failure assuming a reasonable value for the ange of shearing resistance for discontinuities. These will be labelled A, B, C etc.
5. Dividing the road alignment into a number of sections based on the likely instability. These will be labelled 1, 2, 3 etc.
6. Identification of the types of instability that may occur in each section of road.
7. Production of a ranked list of failure mechanisms from most likely to least likely, giving evidence for the choices and listing the discontinuities that contribute to each mechanism.
8. Recommendation of appropriate slope profile to minimize the threat of instability.
9. Formation of a list of questions about the discontinuities that would enable a more detailed design.

1.3 Basic Information

1. A cross section along the centreline of the proposed alignment can be seen in figure 1 on the next page.
2. The orientation of the road centreline is 300°.
3. The ground has an average slope of 10° towards the south all along the alignment.
4. Locally there are small precipitous slopes (2 m - 3 m high) in the sandstone, and there are numerous boulders that have originated from an escarpment to the north of the alignment.
5. It is proposed that the side slopes of the cutting will not be steeper than 80°. The minimum allowable slope (based on land take and the volume of rock to be removed) is 60°.

2 Geology

2.1 Description of rock type and condition

The stratigraphy at the location of the planned cutting consists of a variable depth of sandstone overlying an unknown depth of shale. The rock descriptions and additional information about the two materials are as follows:

Sandstone

"Moderately weak to moderately strong, moderately well cemented greyish yellow calcareous SANDSTONE."

Nearby excavations show that the sandstone weathers relatively rapidly on exposure and becomes prone to frost attack.

250 discontinuities have been observed and recorded at various locations in the sandstone along the proposed alignment. The orientation data are presented in figure 1 on the following page.

In addition to the data presented in figure 1 on the next page, the following additional observations were made for the sandstone:

1. The steeply dipping discontinuities tended to have smooth wavy walls. These discontinuities have a medium to high persistence and a very close to close spacing.
2. The low angle (i.e. low dip) discontinuities have smooth walls and were of high to very high persistence, and a medium spacing. These discontinuities represent bedding planes. There is some evidence of clay infill/clay lining associated with these discontinuities particularly within 50 m of the base of the sandstone.
3. Some of the inclined discontinuities (i.e. intermediate between low angle and steeply dipping) have a medium to low persistence with terminations in other discontinuities. These were found to dip towards the North West and a medium to wide spacing. The walls were generally very rough.
4. Another set of inclined discontinuities were found dipping towards North. These generally had high persistence and smooth walls. This kind of discontinuity was generally absent in the shale.
5. Evidence of seepage was observed for most of the discontinuities..

The clay infill and seepage together suggest that durability problems may occur due to expansion of clay within the discontinuities, leading to disruptive forces within the rock mass:

> "Some clay minerals expand, when wetted, especially those of the montmorillonite groupe, and their increase in volume may create unexpected stress and strain in the ground." (Blyth and Freitas, 1984)

Consequently, steps should be taken to ensure that the clay infill is not subjected to wetting & drying cycles, for example covering the rock surface with shotcrete to prevent water ingress. Additionally, investigation of the clay type within the discontinuities would facilitate a more detailed design that could perform a better assessment of the risk (section section 7 on page 24).

Shale

"Moderately weak to moderately strong, greyish black closely bedded SHALE with occasional nodules of pyrite."

The shale has been found to soften rapidly on exposure and break down into small lumps.

There were insufficient exposures of shale to permit detailed observations of the discontinuities, although the following information was collected:

1. The steeply dipping discontinuities tended to have smooth wavy walls. These discontinuities have a medium to high persistence and a very close to close spacing.
2. The low angle (i.e. low dip) discontinuities have smooth walls and were of high to very high persistence, and a close spacing. These discontinuities represent bedding planes. There is some evidence of clay infill/clay lining associated with these discontinuities particularly within 50 m of the base of the sandstone.
3. In addition to the discontinuity sets shared with the sandstone, the shale supports a set that was not observed in the sandstone. These discontinuities generally had high persistence, close to medium spacing with relatively smooth walls. They have an average dip of 65° and a dip direction of 195°.
4. Evidence of seepage was observed for most of the discontinuities.

In addition to this, it is important to note that the note that the pyrite nodules are a potential durability problem in the shale. Blyth and Freitas (1984) says that pyrite may weather in the presence of acid rain to leave holes where the nodules were previously located, and that: "a shale containing the mineral pyrite, which oxidizes on exposure, may be unsuitable for use in an embankment" because it would "cause the strength of the rock to decrease with time".

Fault

Information from the geological mapping of the area has revealed a fault dipping at 65° towards 330°. The position of the fault is marked on figure figure 1.

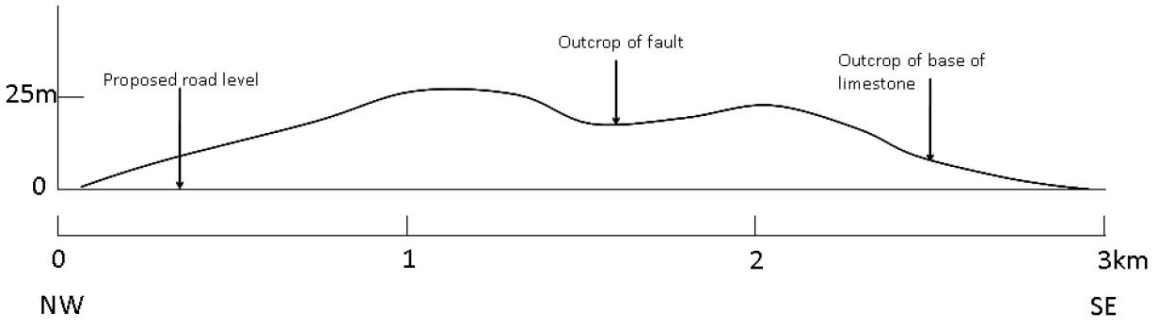

Figure 1: Cross-section along the centreline if the proposed road alignment

2.2 Statistical analysis of discontinuity data

The lower hemispherical projection of the poles to the discontinuities in the sandstone (figure 2) was used along with a counting net to produce figure 3 on the next page, a representation of how many poles are in each ellipse of the Dimitrijevic counting net.

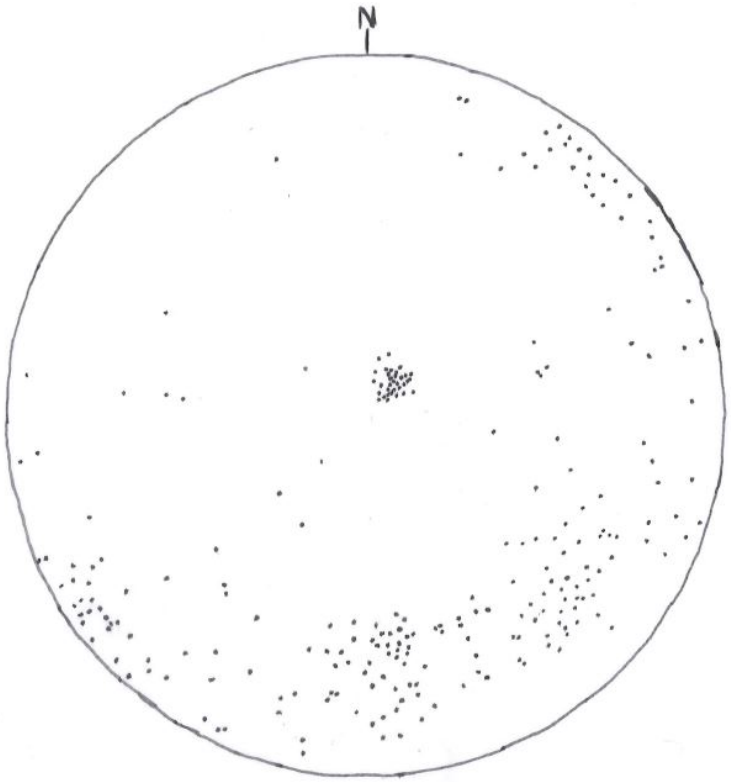

Figure 2: Lower hemispherical projection of poles to discontinuities in the sandstone along the proposed alignment.

This was then used to produce a contoured plot of the distribution of poles per unit area (figure 4 on the following page). The contoured digram allowed a single pole representing each continuity set to be chosen, enabling the construction of a single overlay showing the centres of pole concentrations and great circles for each continuity set (figure 5 on page 6). The fault line and the discontinuity observed in the shale were also marked on the summary overlay. Each pole concentration centre and great circle was labelled with a letter for convenience (A to F) - this is arbitrary, and is not a representation of the severity of the discontinuity set (this was addressed later, in section 2.3 on page 7)

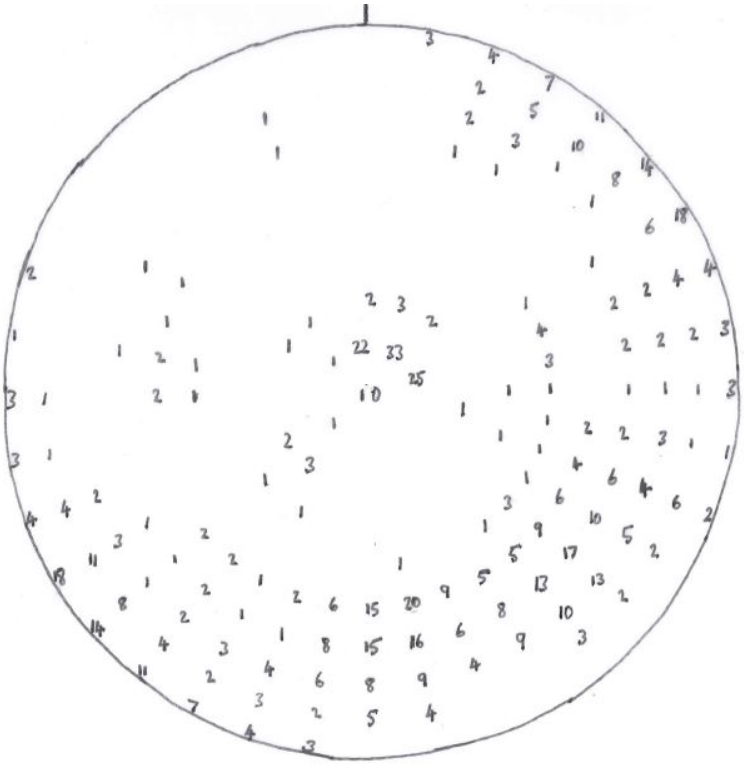

Figure 3: Density distribution of poles per unit area, produced using Dimitrijevic counting net.

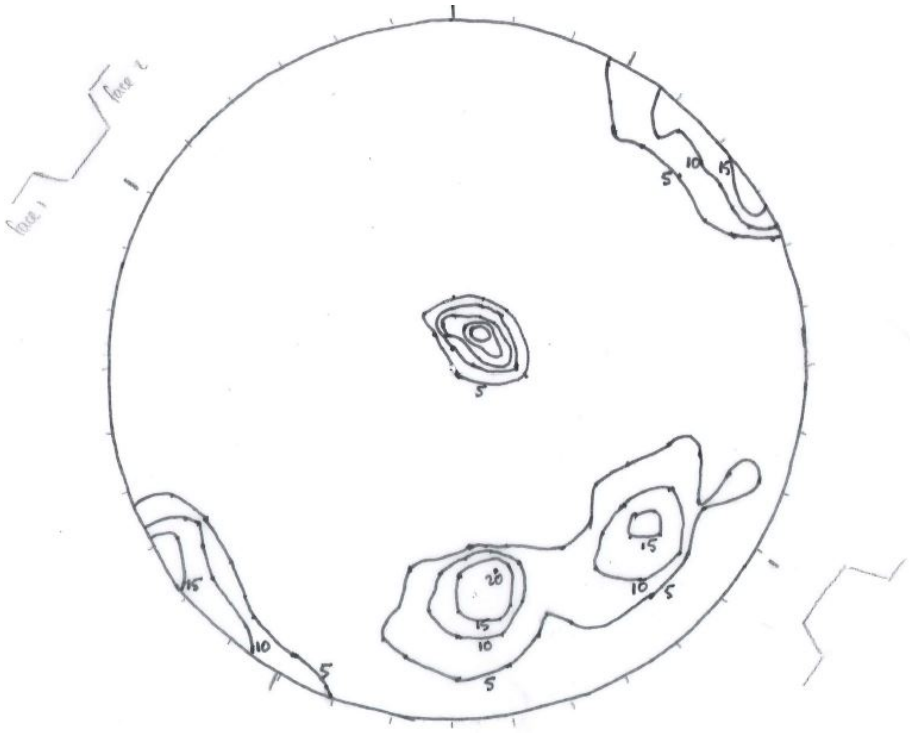

Figure 4: Contoured plot of density distribution.

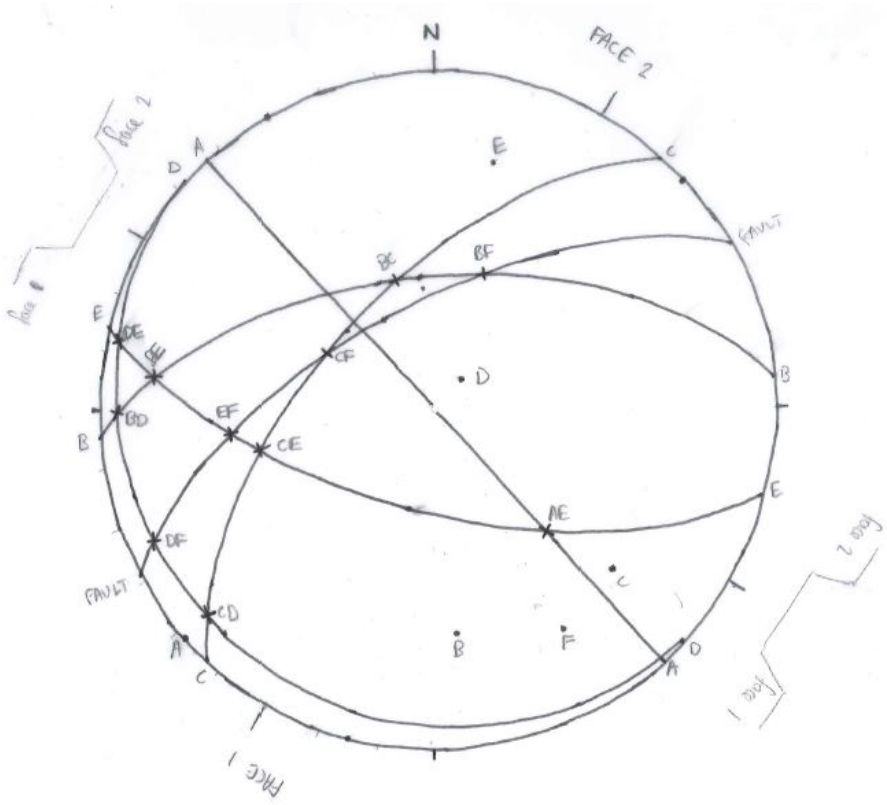

Figure 5: Summary overlay.

2.3 Description of discontinuity sets ranked in order of importance

Set	Average Dip (°)	Dip Direction	Persistence	Concentration	Roughness	Rank
A	90	N/A	High	Very Close	Smooth / Wavy	4
B	58	N	Medium	Medium	Very Smooth	5
C	62	NW	Medium - Low	Medium - Wide	Very Rough	6
D	8	SW	High - Very High	Medium	Very Rough	2
E	65	SW	High	Medium	Smooth	3
F	65	NW	Very High	N/A	N/A	1

Table 1: Description of discontinuity sets ranked in order of importance.

3 Proposed cut slope design - initial choice of profile

The initial cut angle chosen was 70°, mid-way through the permissible range of 60°-80°. This was done because although a steeper angle means that there will be lower land take and excavation of material (and therefore lower costs), it increases the risk of various types of failure because a greater range of dip and dip direction combinations become critical. Doing the analysis at 70° therefore leaves some room for improvements in the final recommendations to either increase or decrease the angle depending on the outcome, and achieve a better solution.

4 Analysis of shear strength tests on discontinuity

According to Wyllie and Mah (2005), the shear strength of a discontinuity surface is dependant on:

1. The applied normal stress.
2. The amount of shear displacement.
3. The combined effects of surface roughness.

After a certain amount of shear displacement, some of the asperities are sheared off, the surface roughness is reduced and the angle of friction for a given normal stress is decreased.

The results from a multi-stage shear box test on discontinuity samples is shown in figure 6 on the next page. Initially, discontinuity surfaces have a peak friction angle of $\phi + i$. According to Wyllie and Mah (2005), if the dilation component is removed, the residual strength of the rock mass can be calculated - this is achieved by recording the horizontal and vertical displacements at peak shear stresses and converting them into i:

$$\frac{dz}{dx} = \tan i$$

After calculating i, the modified shear and normal stresses can be found using the following two equations:

$$\tau_i = (\tau \cos i - \sigma \sin i) \cos i$$

$$\sigma_i = (\sigma \cos i - \tau \sin i) \cos i$$

The angle of friction was then calculated using simple trigonometry and figure 7 on page 9 to be 38°

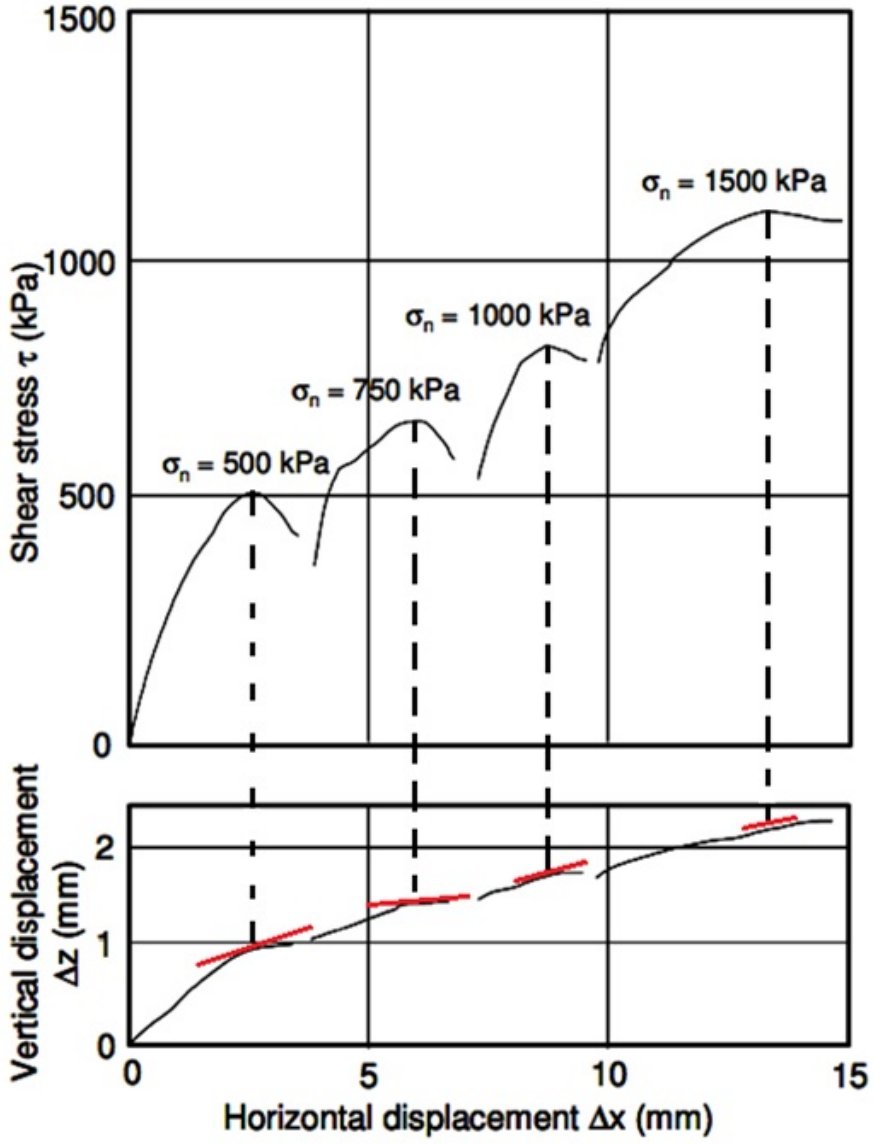

Figure 6: Results from a multi-stage shear box test on discontinuity samples.

Dz mm	**Dx** mm	**i**
0.65	5	0.129
0.25	5	0.050
0.5	5	0.100
0.5	5	0.100

Table 2: Horizontal and vertical displacements at peak stresses.

Peak Shear kPa	**Peak Normal** kPa	**i**	**Residual Shear** kPa	**Residual Normal** kPa
515	500	0.129	509.6	501.2
658	750	0.050	656.5	750.6
816	1000	0.100	810.2	1001.4
1100	1500	0.100	1091.9	1501.9

Table 3: Modified Stresses.

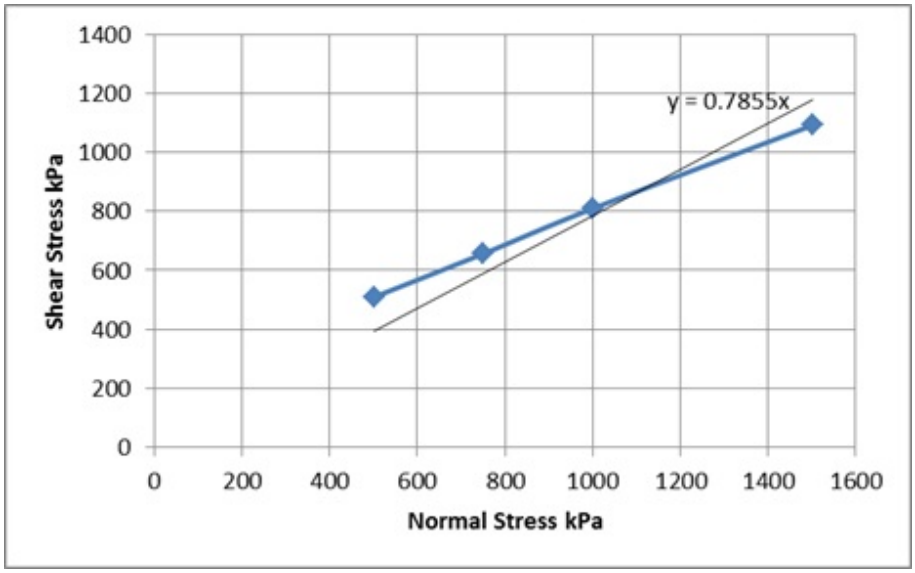

Figure 7: Modified normal stress vs modified sear stress for determination of ϕ.

5 Kinematic feasibility analysis

This section deals with the various possible methods of failure that have been considered, and how the likelihood of each has been assessed.

5.1 Plane Failure Analysis

Plane failure is a risk when the rock contains persistent joints dipping out of the slope face (figure 8). To check for plane failure, an overlay was constructed based on figure 9 on the following page.

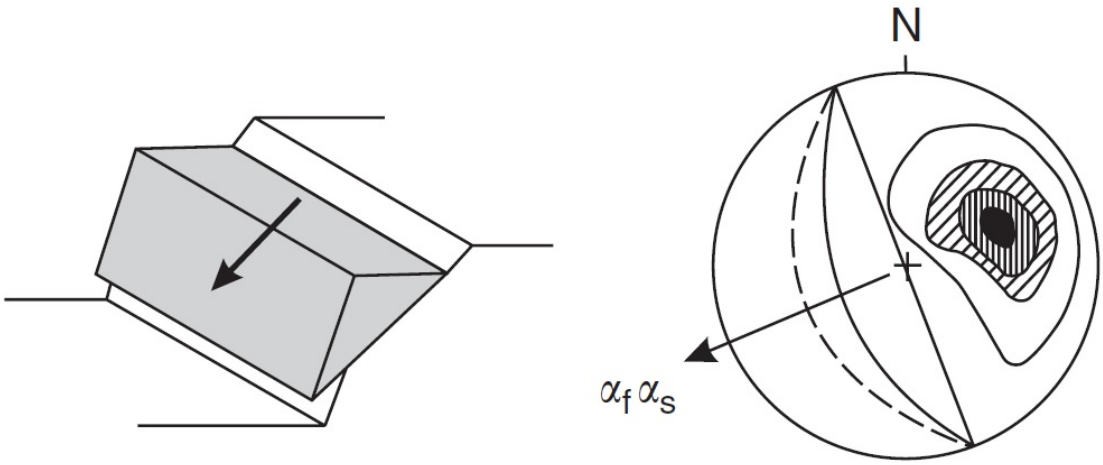

Figure 8: Example of plane failure. α_f is the dip direction of the cut face and α_s is the direction of sliding. The dotted line is the great circle representing the plane that corresponds to the pole concentrations; the solid line is the great circle representing the face (Wyllie and Mah, 2005).

The overlay was then lined up with the cut faces of the proposed excavation, and the centres of pole concentrations were marked on in order to show the risk of plane failure (figure 10 on the next page). Lines representing a cut slope angle of 60°, 70° and 80° are all shown for easy comparison.

Since a pole concentration centre in the region between the inner circle of radius ϕ and the outer line representing the dip of the cut face indicates a risk of plane failure, the overlay shows that:

Face 1

- There would be a risk of plane failure on face 1 if the cut face was vertical (but the maximum permissible angle is 80°).
- No risk of plane failure has been identified for any permissible cut face angle on face 1.

Face 2

- There is a risk of plane failure on face 2 at angles of 70° and 80° if the cut face passes through shale (since pole concentration centre E represents a discontinuity set that is only present in the shale).
- No risk of plane failure at an angle of 60° has been identified.
- In locations that consist solely of limestone above the proposed road level, no risk of plane failure has been identified for face 2.

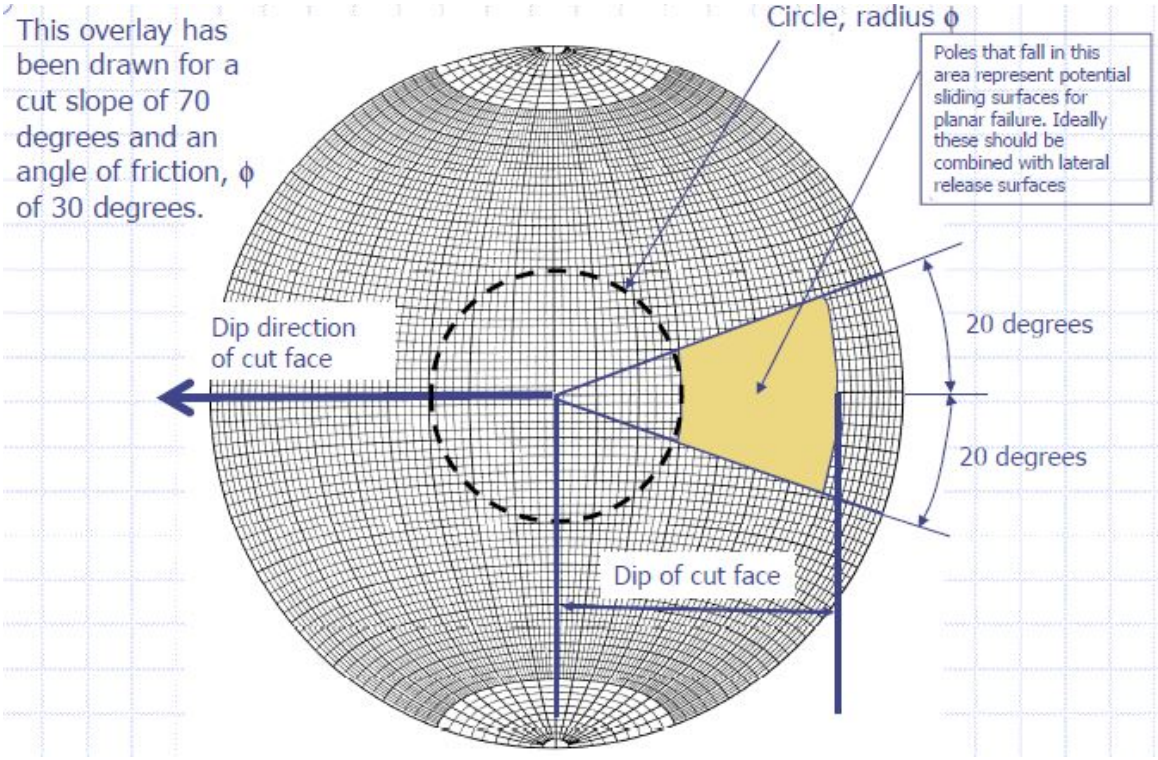

Figure 9: Construction of an overlay for checking plane failure (M. Matthews, 2012a).

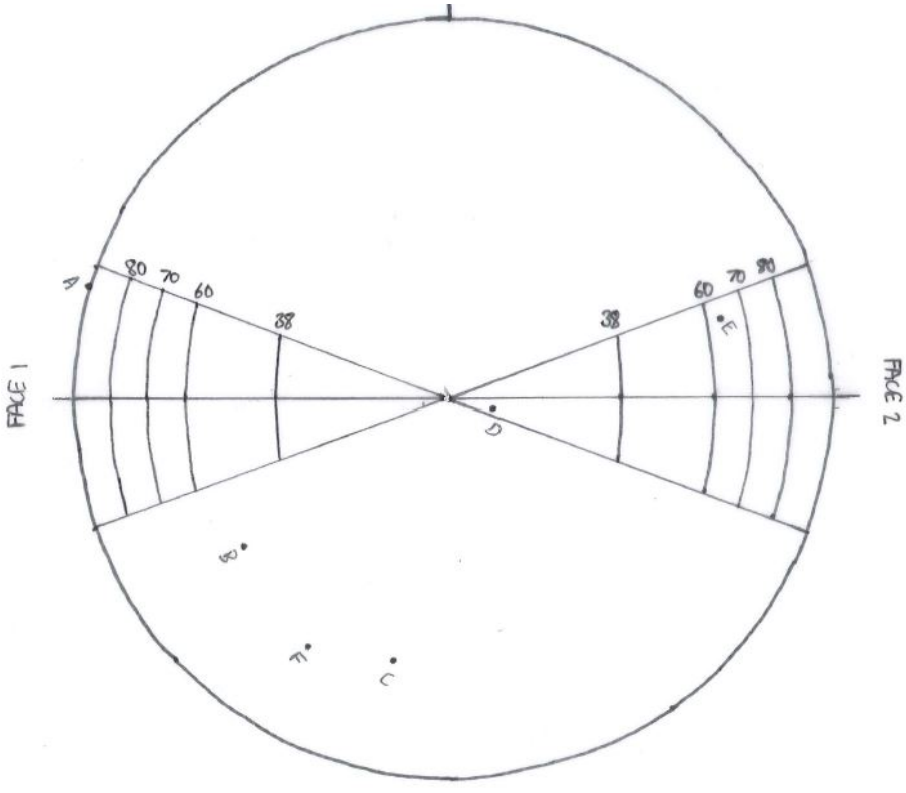

Figure 10: Plane failure analysis for faces 1 and 2 and cut faces angles of 60°, 70° and 80°.

5.2 Wedge Failure Analysis

Wedge failure is a risk when there are two intersecting discontinuities at the necessary dip and dip directions to form a wedge whose line of intersection faces downwards into the cut face (figure 11 on the following page). To check for wedge failure, multiple overlays were constructed based on figure 12 on the next page.

The overlays were then lined up with the cut faces of the proposed excavation, and the centres of pole concentrations and the intersections between great circles, were marked on in order to show the risk of wedge failure (figure 13 on page 14, figure 14 on page 14).

Since an intersection in the zone between the two curves indicates a risk of wedge failure (M. Matthews, 2012b), the overlays show that:

Face 1

- There is a risk of wedge failure at EF (double plane sliding), although this is not a concern as the shale (E) is well below the proposed road level at the position of the fault (F) .
- There is a risk of wedge failure at CE (double plane sliding) in locations where the cut is made in shale.

Face 2

- There is a risk of wedge failure at BC (single plane sliding on B).
- There is a risk of wedge failure at BF (double plane sliding) in the vicinity of the fault.

In order to assess the possible effects of changing the cut slope angle, additional overlays were constructed for 60° and 80°. They showed the following:

Face 1

- When the cut face angle is changed to 60°, there is no change to the failure risks previously identified (figure 15 on page 15).
- When the cut face angle is changed to 80°, an additional failure mechanism is introduced at intersection AE (single plane sliding on E) in locations where the cut is made in shale (figure 17 on page 16).

Face 2

- When the cut face angle is changed to 60°, the failure mechanism previously identified at BC (single plane sliding on B) is no longer a significant risk; the wedge failure mechanism in the vicinity of the fault (BF, double plane sliding) remains a risk (figure 16 on page 15).
- When the cut face angle is changed to 80°, the previously identified failure risks remain unchanged (figure 18 on page 16).

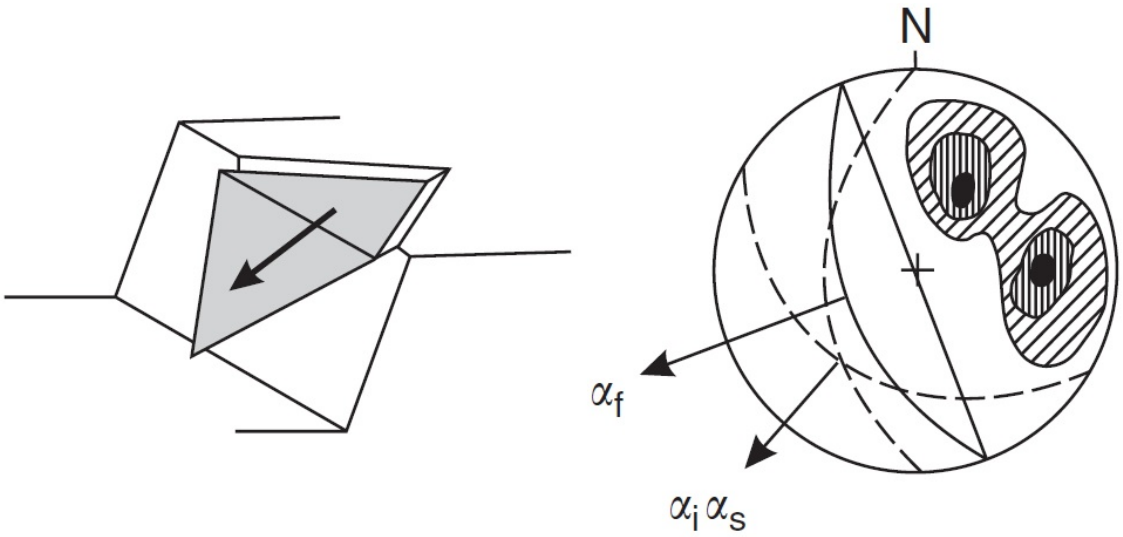

Figure 11: Example of wedge failure. α_f is the dip direction of the cut face, α_s is the direction of sliding and α_i is the dip direction of the line of intersection. The dotted line is the great circle representing the plane that corresponds to the pole concentrations; the solid line is the great circle representing the face (Wyllie and Mah, 2005).

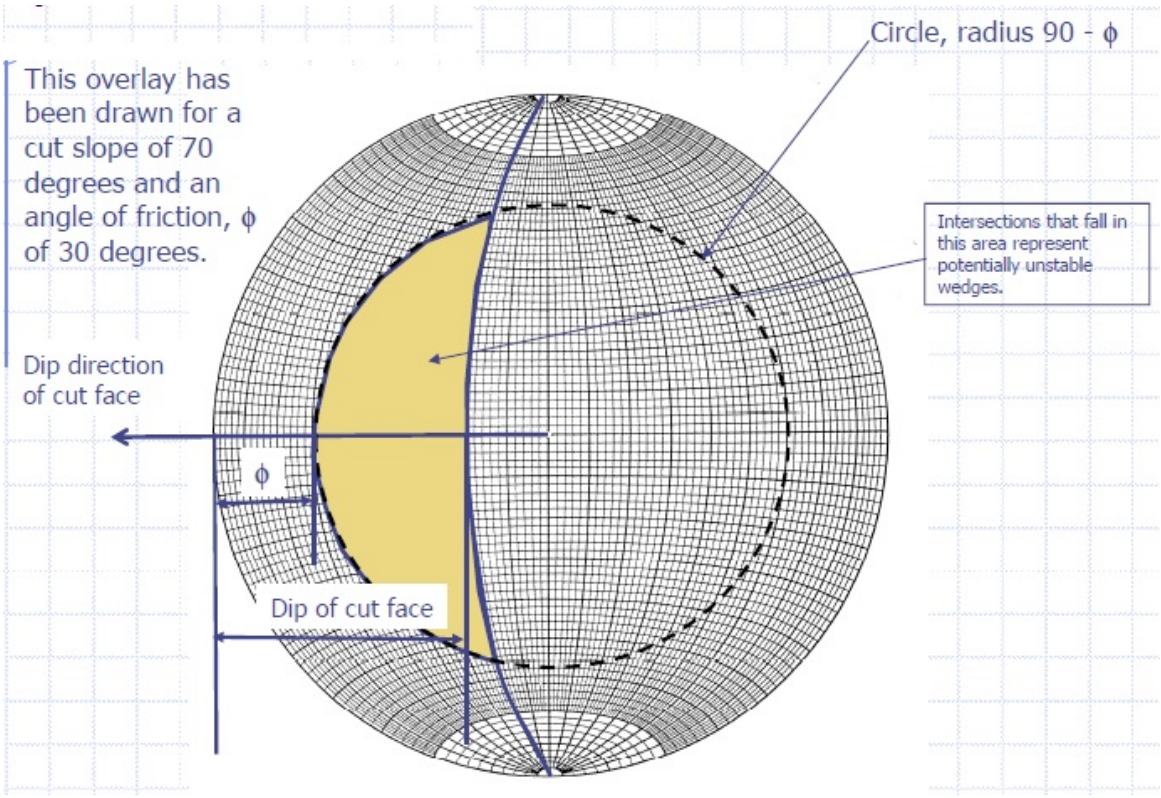

Figure 12: Construction of an overlay for checking wedge failure (M. Matthews, 2012a).

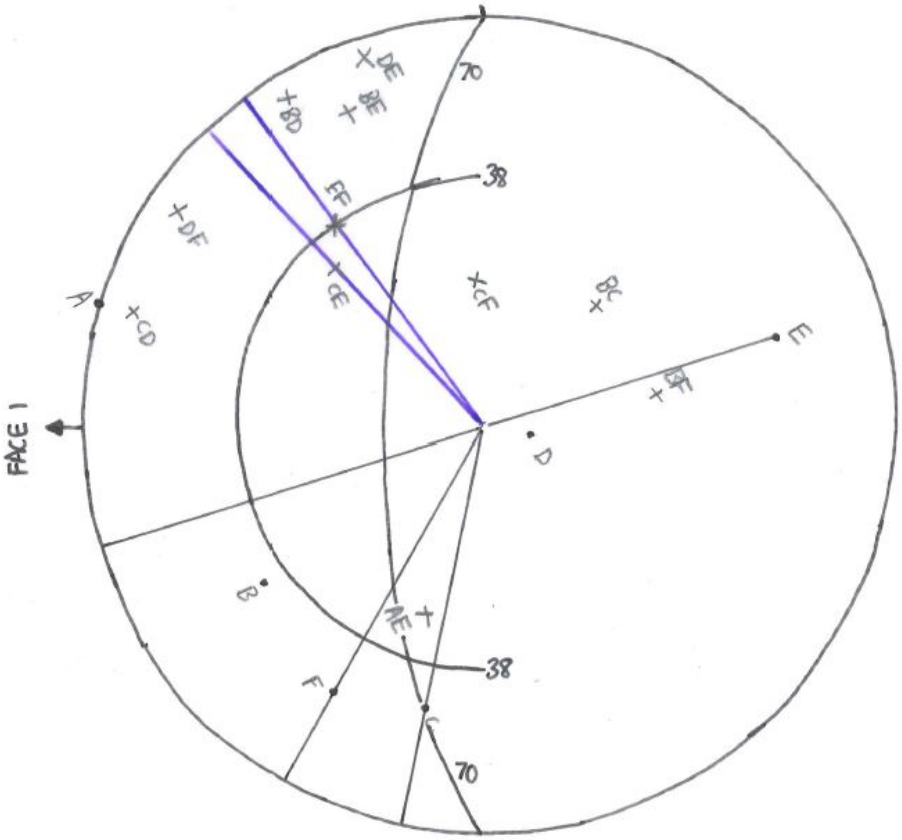

Figure 13: Wedge failure analysis for face 1 and a cut face angle of 70°.

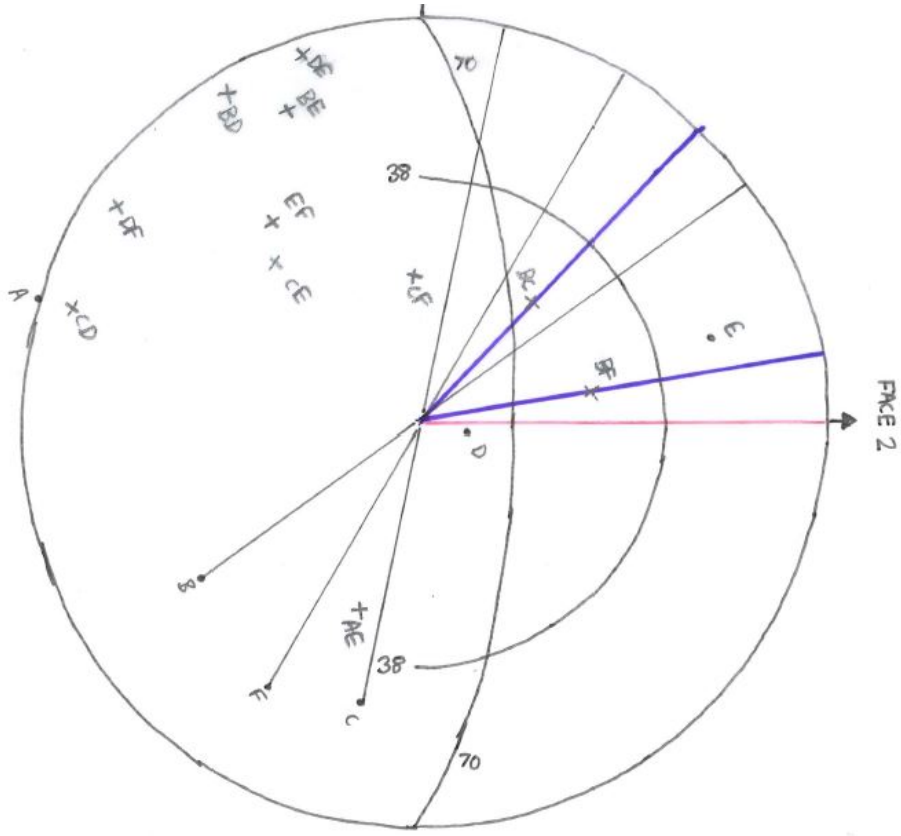

Figure 14: Wedge failure analysis for face 2 and a cut face angle of 70°.

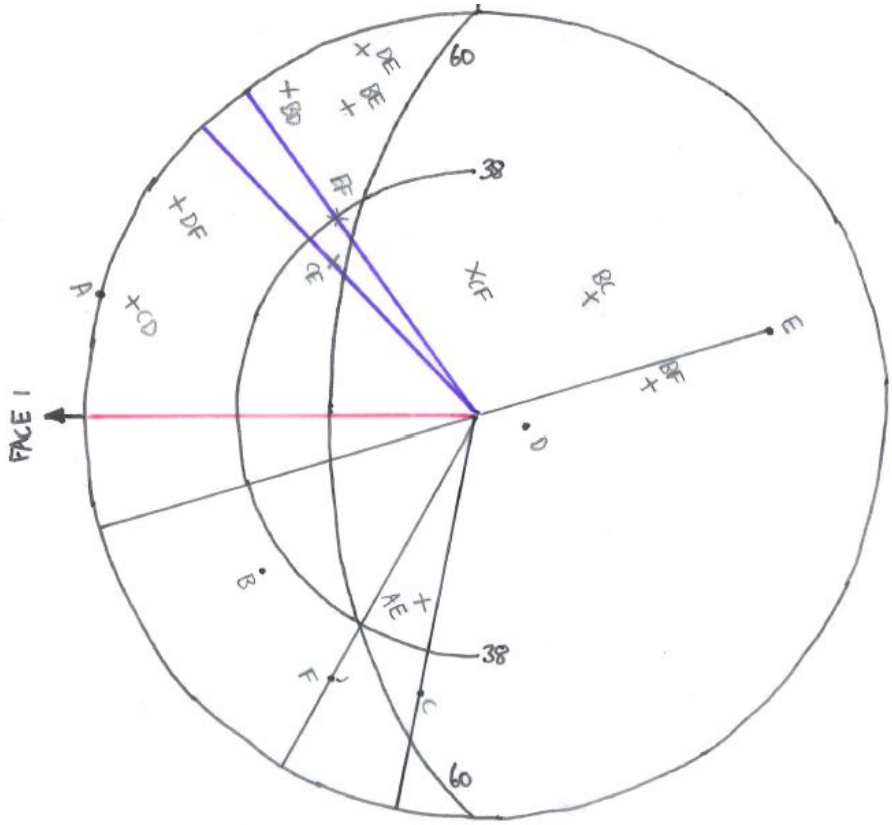

Figure 15: Wedge failure analysis for face 1 and a cut face angle of 60°.

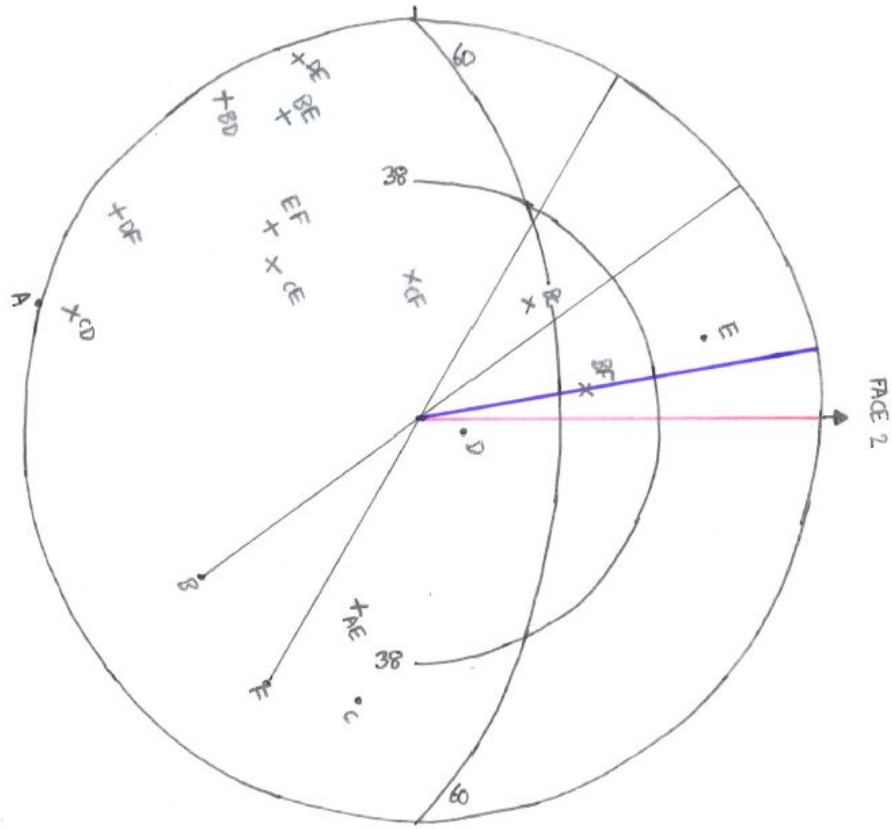

Figure 16: Wedge failure analysis for face 2 and a cut face angle of 60°.

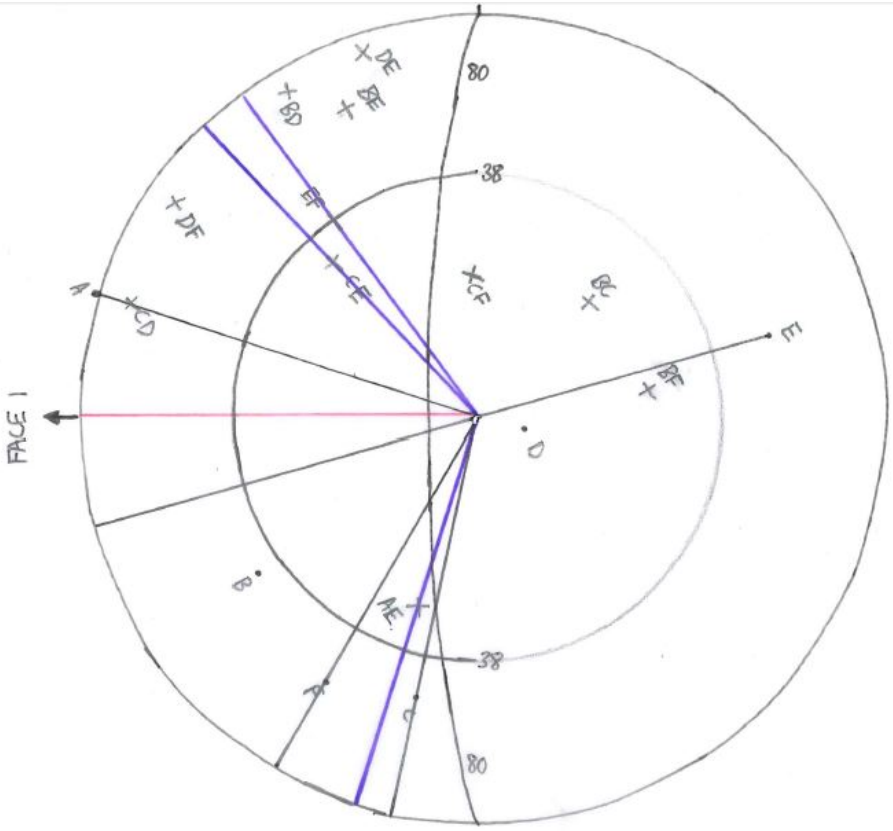

Figure 17: Wedge failure analysis for face 1 and a cut face angle of 80°.

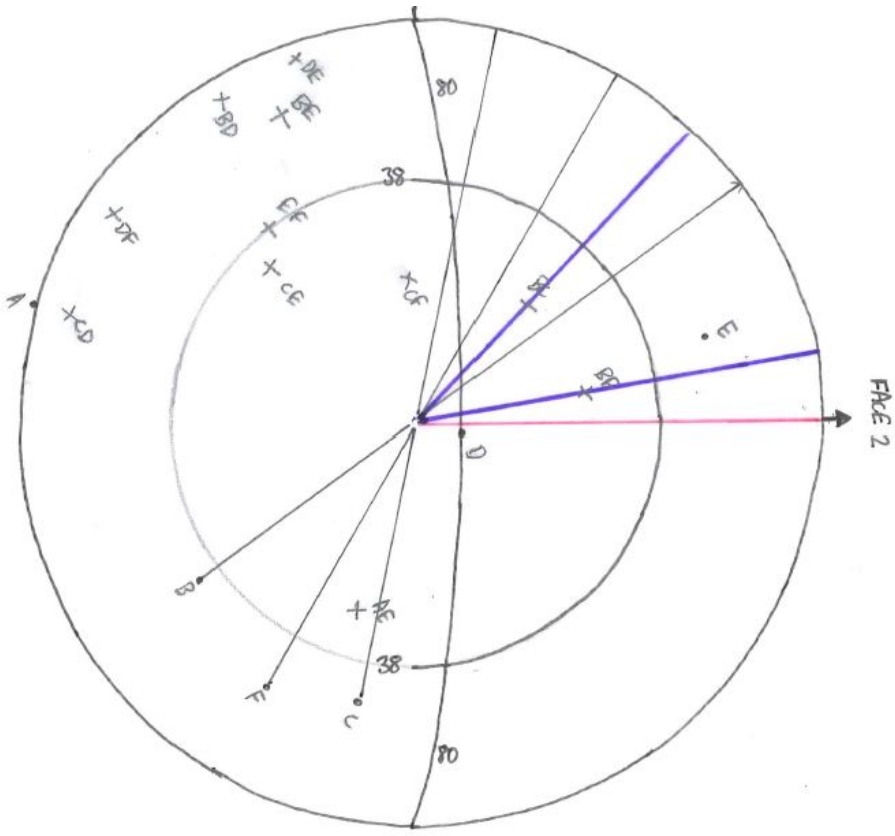

Figure 18: Wedge failure analysis for face 2 and a cut face angle of 80°.

5.3 Toppling Failure Analysis

Toppling failure is a risk when strong rock contains discontinuities with a steep dip angle and a dip direction facing into the cut face (figure 19). To check for toppling failure, multiple overlays were constructed based on figure 20 on the next page and figure 21 on the following page. Because the two types of toppling failure can both be checked using an overlay for block toppling, these are the only overlays that have been constructed. *Block-flexure toppling has not been checked in this analysis*.

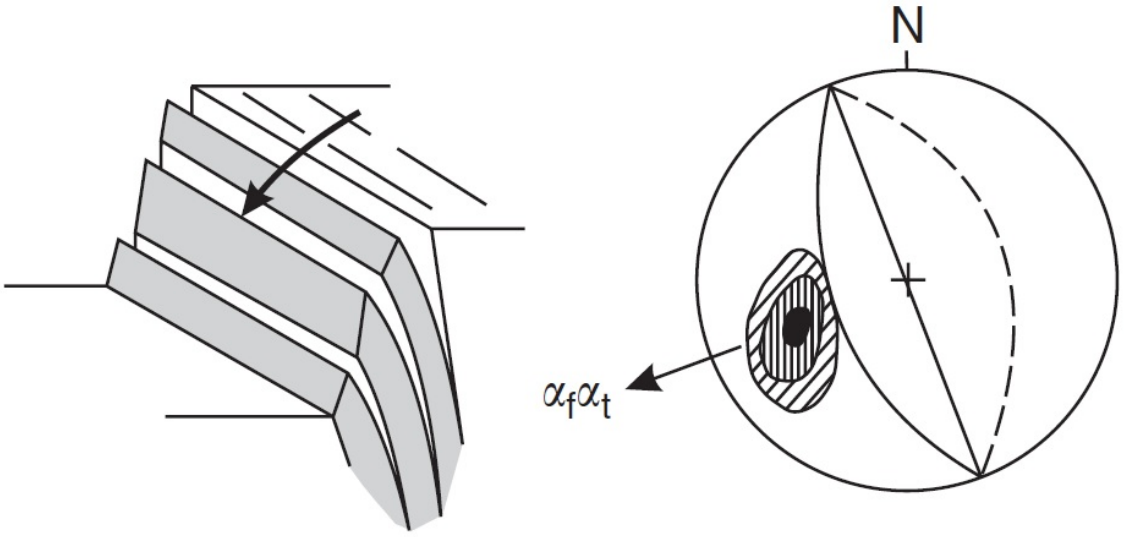

Figure 19: Example of toppling failure. α_f is the dip direction of the cut face, α_t is the direction of toppling. The dotted line is the great circle representing the plane that corresponds to the pole concentrations; the solid line is the great circle representing the face (Wyllie and Mah, 2005).

A centre of pole concentrations within the outer region (marked 'C' on the overlays) combined with a sufficiently small discontinuity set spacing indicates a risk of **flexural toppling** failure (M. Matthews, 2012b). Hence, the overlays for a cut face angle of 70° show that:

Face 1

- There is a risk of flexural toppling involving discontinuity set A, as the concentration (spacing) is "very close" (figure 22 on page 19).

Face 2

- There is a *low* risk of flexural toppling involving discontinuity set E in the shale (figure 22 on page 19): although the centre of pole concentrations falls within region C, the concentration (spacing) is "medium" and may not be sufficiently close to allow a flexural toppling failure mechanism.

In order to assess the possible effects of changing the cut slope angle, additional overlays were constructed for 60° and 80°. They showed the following:

Face 1

- Changing the cut face angle to 60° has no effect on the identified flexural toppling failure mechanisms (figure 24 on page 21).
- Changing the cut face angle to 80° introduces a *low* risk of a new flexural toppling failure mechanism involving discontinuity set B: although the centre of pole concentrations falls within region C, the concentration (spacing) is "medium" and may not be sufficiently close to allow a flexural toppling failure mechanism (figure 26 on page 22).

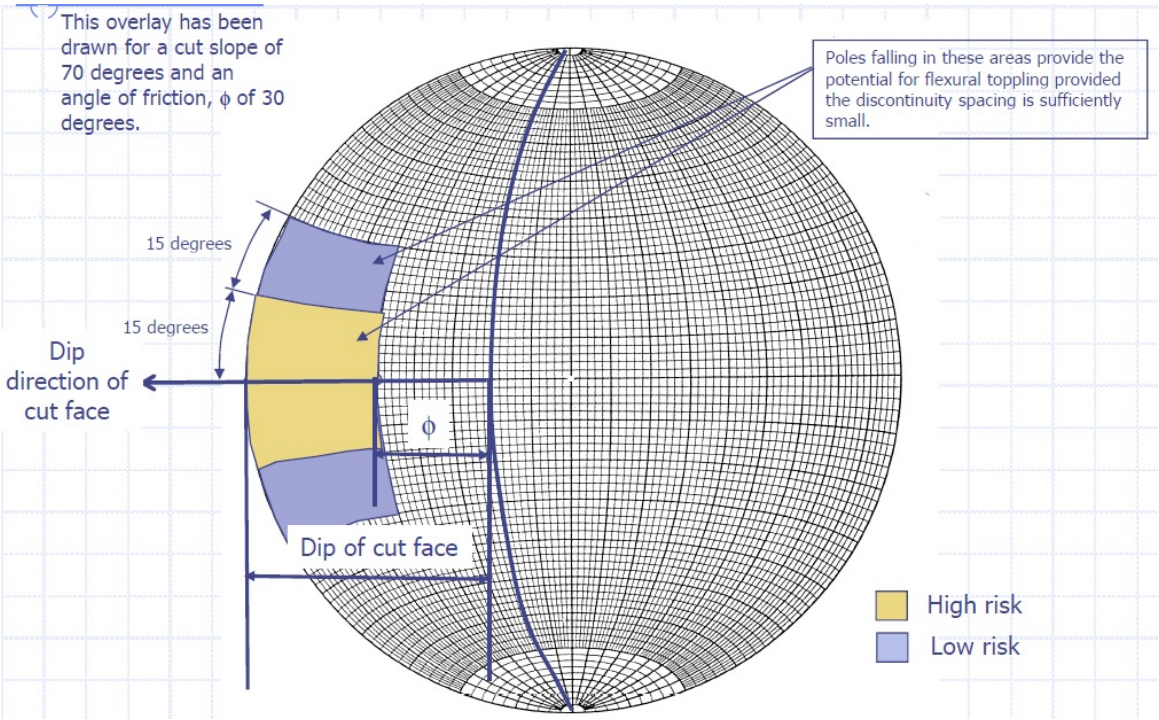

Figure 20: Construction of an overlay for checking fexural toppling failure (M. Matthews, 2012a).

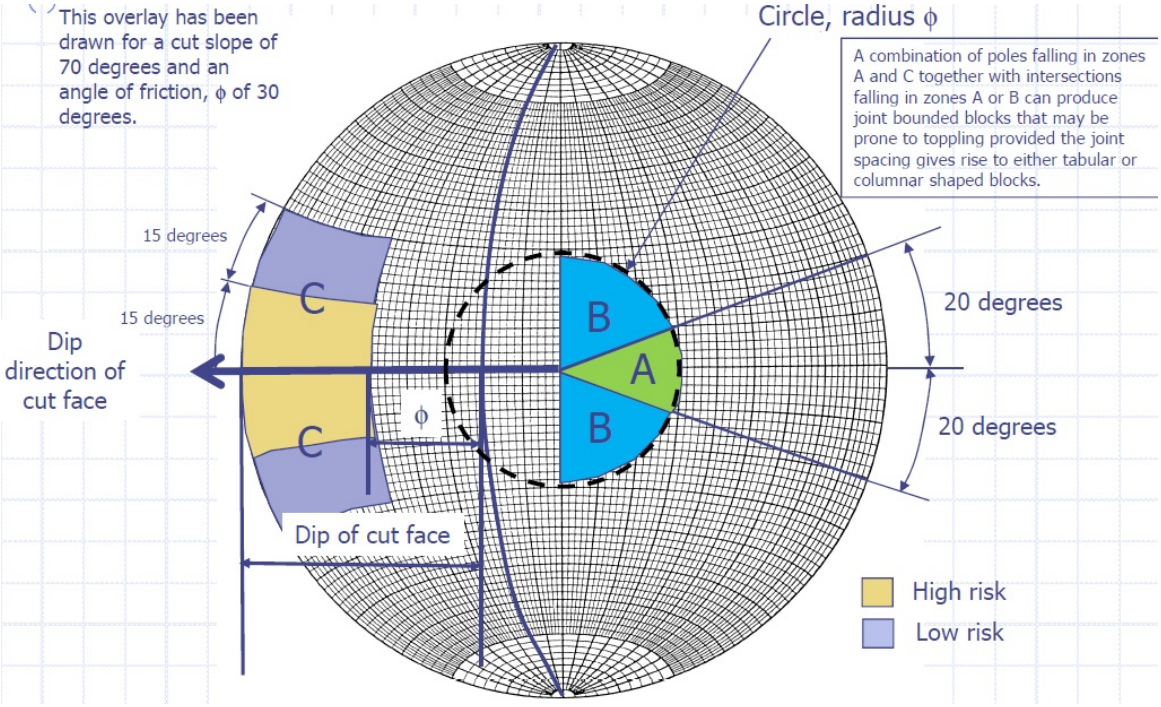

Figure 21: Construction of an overlay for checking block toppling failure (M. Matthews, 2012a).

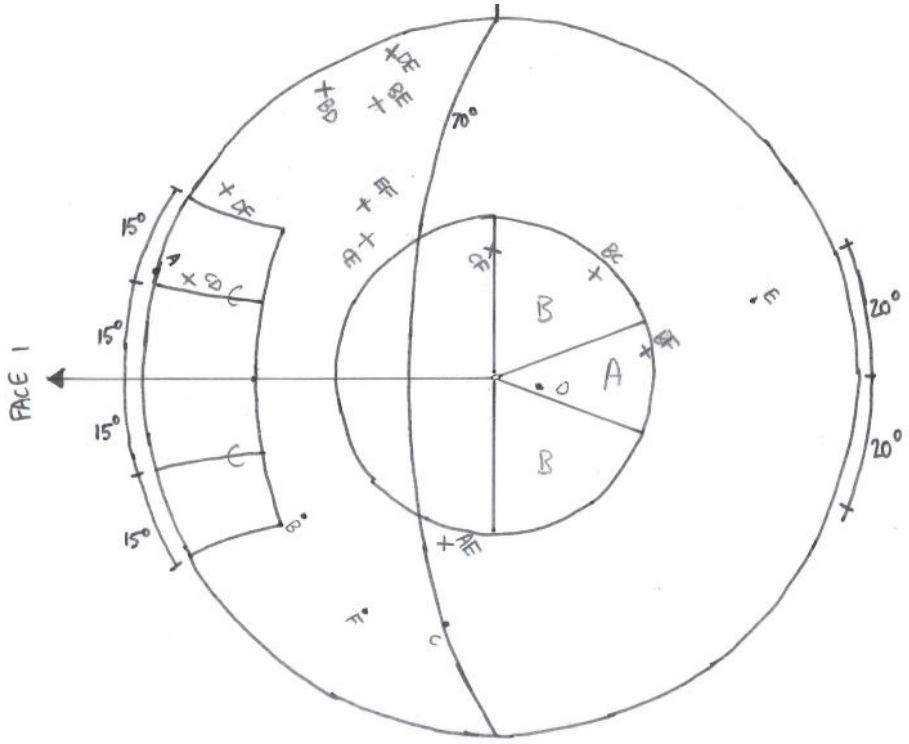

Figure 22: Toppling failure analysis for face 1 and a cut face angle of 70°.

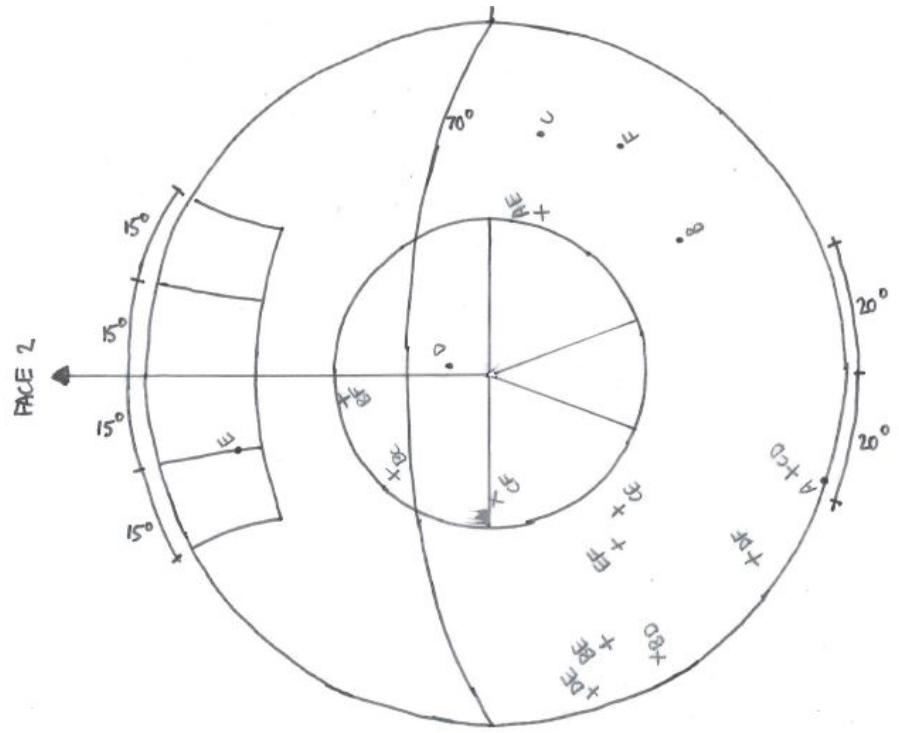

Figure 23: Toppling failure analysis for face 2 and a cut face angle of 70°.

Face 2

- Changing the cut face angle to 60° means that the previously mentioned flexural toppling mechanism involving discontinuity set E is no longer likely (figure 25 on the next page).
- Changing the cut face angle to 80° has no effect on the identified flexural toppling failure mechanisms (figure 27 on page 22).

Having analysed the likelihood of flexural toppling using the toppling overlays, the same overlays will now be used to assess the risk of ***block toppling***.

A centre of pole concentrations within the outer region (marked 'C' on the overlays), combined with a centre of pole concentrations in zone A and intersections in zone A or B, indicates a risk of **block toppling** failure, **if** the joint spacing gives rise to *tabular* or *columnar* block shapes (M. Matthews, 2012b). Hence, the overlays for a cut face angle of 70° show that:

Face 1

- There is a risk of block toppling involving A, D and one of the intersections CF, BC or BF (figure 22 on the previous page). Since the concentration/spacing of discontinuity set is "medium" (table 1 on page 7), this combination of discontinuities is most likely to give rise to columnar blocks and has a *medium risk*, as the chances of a discontinuity falling in the right place is not as high as if the spacing was closer.

Face 2

- No risk of block toppling has been identified for face 2.

Using the overlays for 60° and 80°, the following can be deduced:

Face 1

- Changing the cut face angle to 60° has no effect on the previously identified failure mechanisms for block toppling (figure 24 on the next page).
- Changing the cut face angle to 80° introduces a new block toppling mechanism: B, D and one of the intersections CF, BC or BF (figure 26 on page 22). Since the concentration/spacing of discontinuity set is "medium" (table 1 on page 7), this combination of discontinuities is most likely to give rise to columnar blocks and has a *medium risk*, as the chances of a discontinuity falling in the right place is not as high as if the spacing was closer.

Face 2

- Changing the cut face angle to 60° has no effect on the previously identified failure mechanisms for block toppling (figure 25 on the following page).
- Changing the cut face angle to 80° has no effect on the previously identified failure mechanisms for block toppling (figure 27 on page 22).

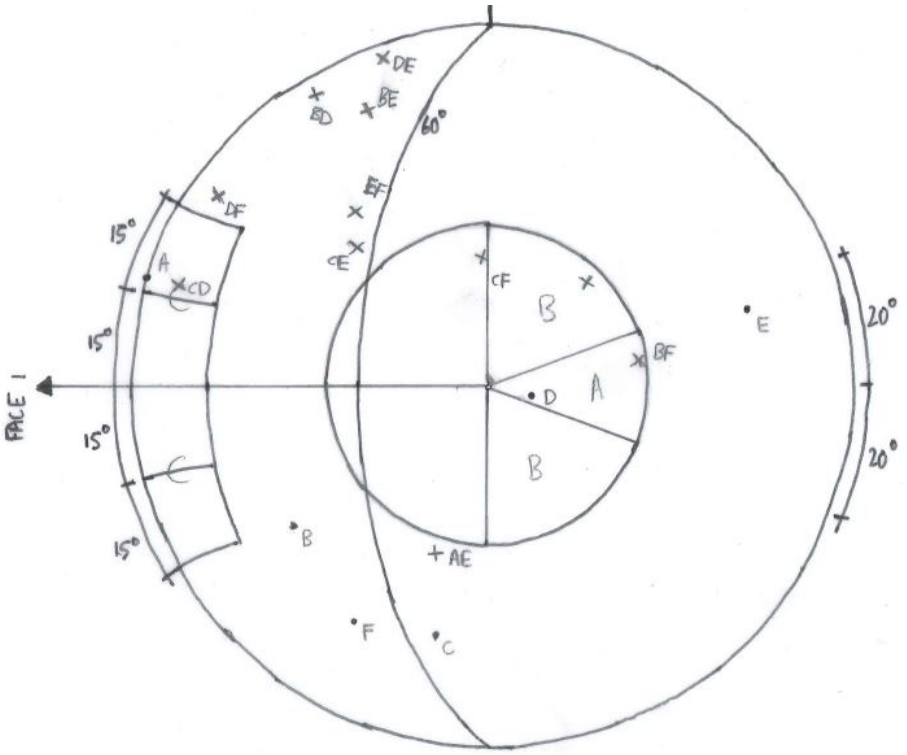

Figure 24: Toppling failure analysis for face 1 and a cut face angle of 60°.

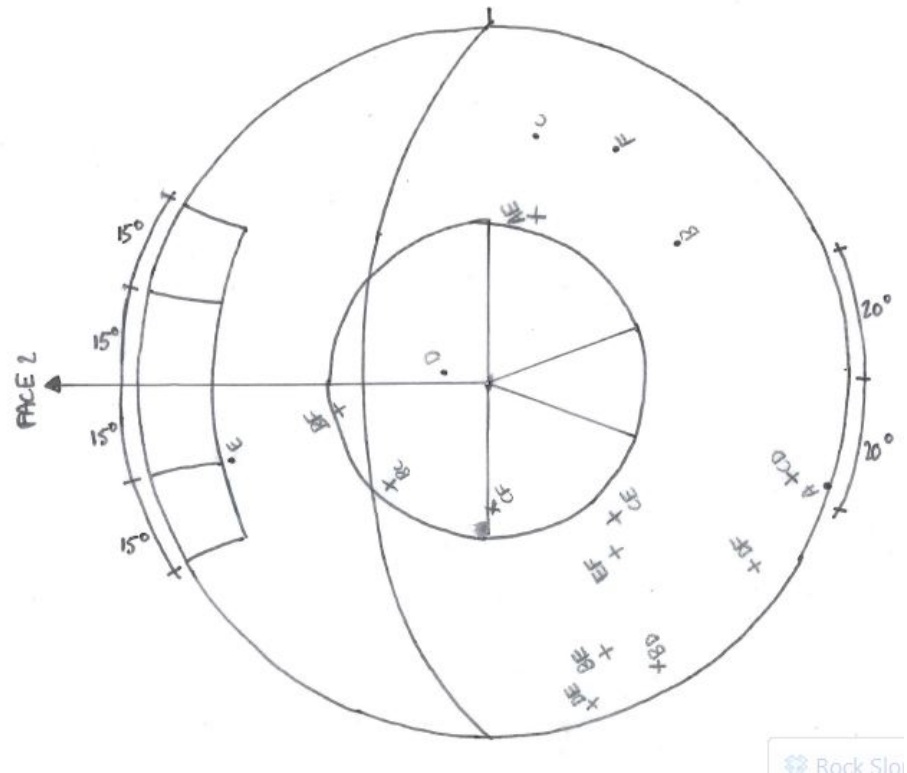

Figure 25: Toppling failure analysis for face 2 and a cut face angle of 60°.

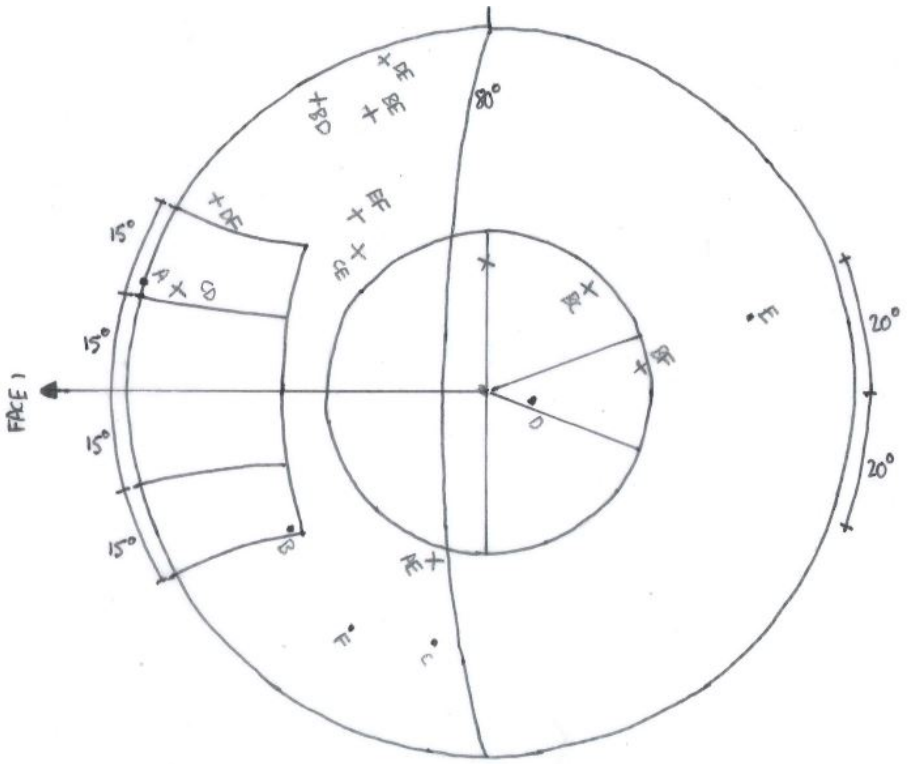

Figure 26: Toppling failure analysis for face 1 and a cut face angle of 80°.

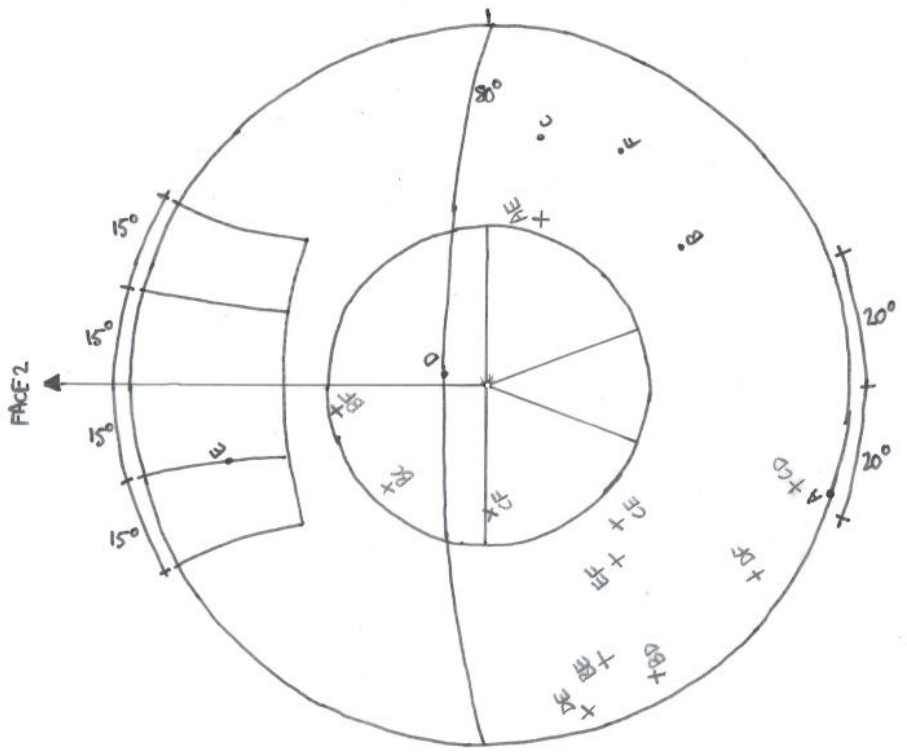

Figure 27: Toppling failure analysis for face 2 and a cut face angle of 80°.

5.4 Summary of Principal Failure Mechanisms in each face

5.4.1 Face 1

A summary of the identified failure mechanisms for face 1 can be seen in table 4, based on the previous discussion and analysis.

	Face cut 60°	**Face cut** 70°	**Face cut** 80°
Plane	None	None	None
Wedge	Shale only	Shale only	Shale only (2)
Flexural Toppling	High risk everywhere	High risk everywhere	High risk everywhere (2)
Block Toppling	Medium risk everywhere	Medium risk everywhere	Medium risk everywhere (2)

Table 4: Summary of identified failure mechanisms and their likelihoods for *face 1* at various cut face angles

5.4.2 Face 2

A summary of the identified failure mechanisms for face 2 can be seen in table 5, based on the previous discussion and analysis.

	Face cut 60°	**Face cut** 70°	**Face cut** 80°
Plane	None	Shale only	Shale only
Wedge	Fault only	Everywhere and fault	Everywhere and fault
Flexural Toppling	None	Low risk Shale	Low risk Shale
Block Toppling	None	None	None

Table 5: Summary of identified failure mechanisms and their likelihoods for *face 2* at various cut face angles

6 Suggested changes to cut face profiles that may reduce or eliminate failure mechanisms

This section deals with modifications to the original selection of a 70° cut face in order to either:

- Save money by making the angle steeper where it has no effect on the risk of failure (lower land take and excavation costs).
- Minimise the likelihood of different failure mechanisms to eliminate or reduce as far as possible the need for remedial works for residual failure mechanisms.

The choices are outlined in table 6 on the following page.

The cut angles for face 1 were chosen based on the following information. Firstly, table 4 suggests that the difference in failure mechanisms for cut angles between 70° and 80° is the number of possible mechanisms but not the severity (since the flexural toppling mechanism involving set A is a higher risk than the mechanism involving set B due to the spacing). Since it is not possible to completely remove the risk by choosing an angle of 60°, some remedial works will be required to stabilise the face against flexural and block sliding in all locations (and wedge failure in section 5) regardless of the number of possible mechanisms, so a steeper angle was chosen to minimise the cost of cutting and land take.

Section No.	Chainage (km)	Face 1 angle (°)	Face 1 residual risks	Face 2 angle (°)	Face 2 residual risks
1	0 - 0.75	80	Flexural, Block	60	N/A
2	0.75 - 1.5	80	Flexural, Block	60	N/A
3	1.5 - 1.75	80	Flexural, Block	60	Wedge
4	1.75 - 2.5	80	Flexural, Block	60	N/A
5	2.5 - 3	60	Wedge, Flexural, Block	60	N/A

Table 6: Summary of chosen cut face angles and the residual risks at that angle.

The cut angles for face 2 were chosen based on the following information. Firstly, table 5 on the preceding page shows that there is a risk of wedge failure in all locations at 70° but only near the fault (section 3) at 60°. Secondly, changing the angle from 70° to 60° also removes the plane and flexural toppling failure mechanisms in the shale. Both of these reduce the need for expensive work to address residual risks. However, it is noted that for sections 1 to 4 it could be cheaper to provide some kind of stabilisation against wedge failure than to cut out more rock and use more land, therefore a cost-benefit analysis should be undertaken in order to investigate whether it would be worth using a cut angle of 80° in these sections.

7 Recommendations for further investigation

Since the durability of the sandstone depends on whether the clay in the discontinuities belongs to the montmorillionite group or contains similar expansive minerals (as mentioned in section 2.1 on page 2), further testing should be undertaken to investigate its properties to decide whether a lower the angle ϕ should be used.

Investigation of how the water table changes (i.e. is there seasonal variation?) with the use of in situ tests could also help assess the risk of durability issues affecting the slope stability through interaction with pyrite in the shale or the clay in the sandstone.

Detailed testing on severely weathered sections of the limestone and shale should be undertaken to determine the most sensible value to use for ϕ, enabling the overlays to be redrawn for this as a worst case to see what effect changing ϕ has on the possible failure mechanisms.

Should the ϕ sensitivity analysis show that an accurate estimate is essential, an in-situ plate loading test could be used to get a better value, however such a test would be very expensive and would probably not be justifiable unless small changes in the value of ϕ have a large effect on the cost of construction.

As mentioned previously, a cost-benefit analysis would enable a slope angle to be chosen based on the cost of more cutting and land take against the cost of stabilisation work.

References

Blyth, F G H and M H de Freitas (1984). *A Geology for Engineers*. 7th ed. GB: Elsevier Butterworth-Heinemann. ISBN: 0-7131-2882-8.

Clayton, C R I, N E Simons, and M C Matthews (1995). *Site Investigation*. 2nd ed. Blackwell Science Inc. ISBN: 0632029080.

Dimitrijevic, M D and R S Petrovic (1965). *The use of sphere projection in geology*. Tecnhical report. Ljubljana: Geoloski Zavod.

Matherson, G D (1983). *Rock stability assessment in preliminary site investigations - graphical methods*. TRRL Report LR 1039. Crowthorne, Berks: Transport Research Laboratory.

Matthews, Marcus (2012a). *Classification of Discontinuities and Construction of Stability Overlays*. Lecture Slides. Guildford, Surrey: University of Surrey.

— (2012b). *Kinematic Feasibility Analysis*. Lecture Slides. Guildford, Surrey: University of Surrey.

Wyllie, Duncan C and Christopher W Mah (2005). *Rock Slope Engineering. Civil and Mining*. Based on the third edition by E Hoek and J Bray. 4th ed. Spon Press. ISBN: 0-203-49908-5.